Spectrum of Engineering Sciences

ISSN (e) 3007-3138 (p) 3007-312X Volume 4, Issue 3, 2026

SYNTHESIS AND CHARACTERIZATION OF GRAPHENE OXIDE-POLYANILINE-SODIUM FLUORIDE HYBRID COMPOSITES: AC IMPEDANCE AND ELECTROCHEMICAL PROPERTIES FOR SOLID-STATE BATTERY APPLICATIONS

Aiman[1], Hassan Saleemi[*2], Fatima Muneer[3], Rida Zameer[*4], Iqra Siraj[5], Muhammad Junaid Abdullah[6]

[1]*School of Chemistry, University of the Punjab, Lahore*
[*2]*University of Punjab Institute of Chemical Engg & Technology (I. C. E. T Lahore -54590 Pakistan.*
[3]*Department of Chemistry, University of Management and Technology, Lahore*
[*4]*Department of Chemistry, Hazara University, Mansehra-21300, Khyber Pakhtunkhwa, Pakistan*
[5]*Department of Physics, Hazara University, Mansehra-21300, Khyber Pakhtunkhwa, Pakistan*
[6]*Department of Chemistry, Hazara University, Mansehra-21300, Khyber Pakhtunkhwa, Pakistan*

[1]aimanwaqas.chem@gmail.com, [*2]saleemih72@gmail.com, [3]fatimamuhammadmuneer@gmail.com, [*4]ridazameer04@gmail.com, [5]iqrasiraj696@gmail.com, [6]mjunaidabdullah56@gmail.com

DOI:https://doi.org/10.5281/zenodo.22706527

Keywords
Solid-state sodium battery, Gel polymer electrolyte, Graphene oxide, Polyaniline, Electrochemical impedance spectroscopy.

Article History
Received: 30 January 2026
Accepted: 15 March 2026
Published: 31 March 2026

Corresponding Author: *
Hassan Saleemi
Rida Zameer

Abstract

Developing safe, high-performance solid-state sodium batteries require engineering advanced electrolyte matrices capable of sustaining rapid ion-transport kinetics and enduring interface stability. A novel ternary Graphene Oxide-Polyaniline-Sodium Fluoride (GO-PANI-NaF) hybrid composite was synthesized via collaborative solution blending, chemical polymerization, and rapid thermal-shock reduction. FTIR analysis confirmed strong interfacial hydrogen bonding and chemical coupling across the functionalized networks, while XRD profiles confirmed the coexistence of amorphous polymer chain regions and crystalline NaF domains (33.65°, 38.95°, and 56.20°). SEM imaging revealed highly exfoliated, porous carbon sheets covered with micro-granular PANI-NaF clusters, creating optimized pathways for ionic conduction. Electrochemical impedance spectroscopy demonstrated that internal charge-transfer resistance drops from an initial 1450 Ω to 1100 Ω after activation cycles. Cyclic voltammetry verified outstanding redox reversibility with mirrored anodic and cathodic peaks at 3.4 V and 3.3 V, respectively. Galvanostatic testing delivered a peak specific discharge capacity of 111 mAh g^{-1} at 0.47 mA cm^{-2}, while retaining an impressive capacity of 61 mAh g^{-1} under an aggressive current load of 9.940 mA cm^{-2}. The composite electrode maintained a steady Coulombic efficiency plateau near 98% over 100 cycles, showcasing structural resilience and exceptional utility for next-generation solid-state sodium battery technologies.

Spectrum of Engineering Sciences

ISSN (e) 3007-3138 (p) 3007-312X Volume 4, Issue 3, 2026

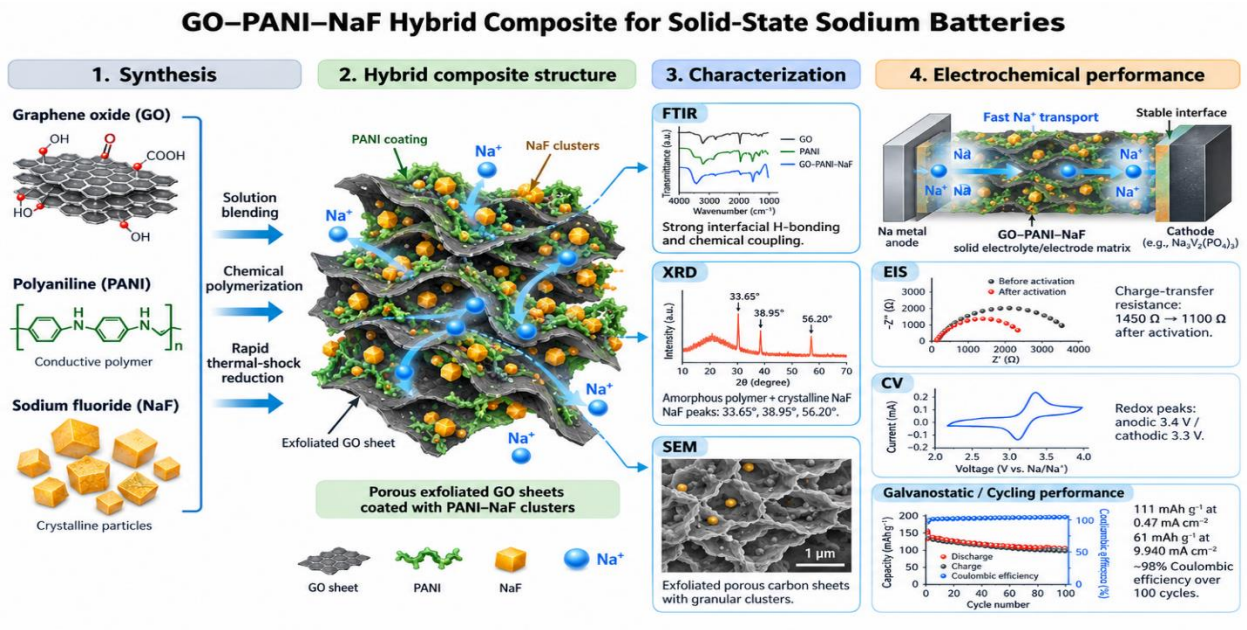

Graphical Abstract

1. INTRODUCTION

The rapid depletion of fossil fuels coupled with escalating global environmental concerns has accelerated the transition toward clean, sustainable, and renewable energy technologies [1]. Among various energy storage systems, secondary batteries have emerged as indispensable components powering portable electronic devices, electric vehicles (EVs), and smart grid applications. For decades, lithium-ion batteries (LIBs) have dominated the market due to their high energy density and mature manufacturing infrastructure [2]. However, the geographic concentration and skyrocketing costs of raw lithium reserves pose severe risks to long-term sustainability. Consequently, sodium-ion batteries (SIBs) have gained global prominence as a promising alternative [3]. Sodium is environmentally abundant, cost-effective, and shares highly analogous intercalation chemistry with lithium, making it ideal for next-generation, large-scale electrical grids [4].

Despite their enormous potential, conventional sodium-ion configurations are hindered by the use of volatile organic liquid electrolytes. These liquid matrices present severe safety vulnerabilities, including volatile leakage, flammability, dendrite propagation, and catastrophic thermal runaway under extreme physical or electrochemical stress [5-7]. To mitigate these hazards, research has pivoted toward solid-state batteries utilizing solid polymer electrolytes (SPEs) or gel polymer electrolytes (GPEs). Gel polymer electrolytes combine the high ionic conductivity and superior electrode wetting properties of liquid variants with the mechanical structural integrity and leak-proof characteristics of solid matrices. Generally, conducting polymers serve as excellent structural frameworks for these gel configurations due to their unique macromolecular flexibility and ability to participate in localized charge-transport dynamics [9-11].

Among various conducting hosts, polyaniline (PANI) is widely investigated due to its exceptional environmental stability, tunable electrical properties, easy synthesis, and controllable redox behavior. PANI forms an amorphous network that facilitates structural chain relaxation, which assists local ion movement. However, pure polymer matrices frequently suffer from low room-temperature ionic conductivity and weak mechanical thresholds under continuous battery

cycling [12]. To resolve these challenges, modern material strategies focus on fabricating organic-inorganic hybrid nanocomposites by embedding zero- or two-dimensional nanofillers into the host polymer framework [13]. Graphene oxide (GO), a functionalized two-dimensional carbon derivative, represents an exceptional choice for structural reinforcement. GO nanosheets are highly decorated with surface oxygenated functional groups, including hydroxyl, epoxy, and carboxyl networks [14]. These oxygen clusters interact strongly with the host polymer chains, effectively disrupting natural polymer crystallization, reducing the glass transition temperature and generating multi-dimensional amorphous channels that accelerate ion migration. Concurrently, incorporating a highly pure, active inorganic salt like sodium fluoride (NaF) provides a robust concentration of mobile sodium ions Na^+, which serves as the primary charge carrier required for driving efficient electrochemical cell configurations [15-28].

Despite the theoretical advantages of blending polymers with carbon nanosheets, current research faces a persistent bottleneck: solid-state gel electrolytes typically demonstrate inadequate room-temperature ionic conductivity and poor structural stability during prolonged cycling due to severe nanofiller agglomeration and poor interfacial compatibility between the host polymer and the inorganic salt. While many studies isolate binary configurations such as PANI-NaF or GO-PANI, there remains a critical research gap concerning the development and comprehensive characterization of an integrated ternary Graphene Oxide-Polyaniline-Sodium Fluoride (GO-PANI-NaF) hybrid network engineered specifically for solid-state sodium battery applications. The precise structural synergy, molecular cross-linking, AC conductivity mechanics, and thermal degradation limits of this ternary formulation remain unexplored. This research addresses this gap by synthesizing a highly homogeneous GO-PANI-NaF hybrid matrix using a controlled solution-blending and thermal-shock reduction methodology. By thoroughly analyzing its crystal structure, surface morphology, dynamic AC conductivity, and long-term electrochemical capacity decay profiles, this study establishes a novel, stable, and highly conductive gel electrolyte architecture that overcomes traditional interface limitations, paving the way for safer and more efficient next-generation solid-state sodium storage devices.

2. EXPERIMENTAL

2.1 Chemicals and Reagents

All high-purity chemical reagents were purchased from Sigma-Aldrich and utilized as received without further purification. The foundational materials include Natural Graphite Powder (Mw: 12.01 g/mol, 99.0% purity) and Aniline Monomer (Mw: 93.13 g/mol, 99.5% purity). Sodium Fluoride (NaF) (Mw: 41.99 g/mol, 99.0% purity) was sourced as the active sodium-ion provider, while Potassium Persulfate $K_2S_2O_8$ (Mw: 270.32 g/mol, 99.0% purity) served as the polymerization initiator. For the oxidative framework, Sulfuric Acid H_2SO_4 (Mw: 98.08 g/mol, 98% purity), Sodium Nitrate $NaNO_3$ (Mw: 84.99 g/mol, 99.0% purity), Potassium Permanganate $KMnO_4$ (Mw: 158.03 g/mol, 99.0% purity), and Hydrogen Peroxide H_2O_2 (Mw: 34.01 g/mol, 30% aqueous solution) were utilized. Acetic Acid CH_3COOH (Mw: 60.05 g/mol, 99.7% purity) was employed to prepare the solvent matrices.

2.2 Synthesis of Graphene Oxide (GO)

raphene oxide (GO) was synthesized via a modified Hummers' method from pristine graphite powder, followed by a thermal shock reduction process to yield reduced graphene oxide (rGO). Initially, 0.5 g of graphite was dispersed in 23 mL of concentrated H_2SO_4 under constant stirring, followed by the addition of 0.5 g of $NaNO_3$. To initiate controlled oxidation, the mixture was transferred to an ice bath environment, where 3 g of $KMnO_4$ was added slowly to prevent exothermic runaway. The solution was subsequently heated, and deionized water was added to induce hydrolysis. The

ISSN (e) 3007-3138 (p) 3007-312X Volume 4, Issue 3, 2026

oxidation reaction was quenched by introducing 50 mL of H_2O_2, resulting in a distinct color change. The suspension was purified via centrifugation at 3000 rpm and washed repeatedly before being dried in a stove at 40 °C for 48 hours to obtain structured GO. Finally, to produce highly conducting rGO, the dried GO underwent rapid thermal exfoliation in an oven at 350 °C for 30 seconds. The resulting fluffy, dark product was crushed into a fine powder and collected (Figure 1b) for subsequent gel polymer electrolyte formulation.

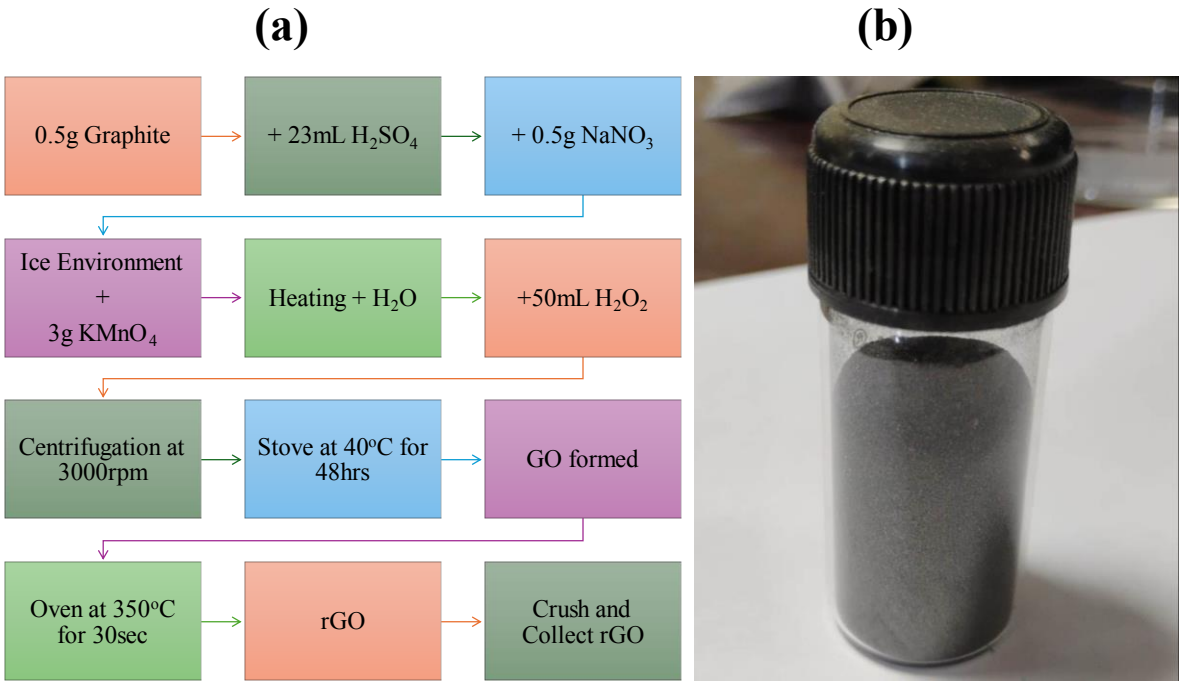

Figure 1: Synthesis of Graphene Oxide(GO) (a) Flow chart (b) Snap taken during GO Synthesis

2.3 Synthesis of Graphene Oxide-Polyaniline (GO-PANI) composite

The Graphene Oxide-Polyaniline (GO-PANI) nanocomposite was fabricated through a collaborative solution blending and thermal treatment process. Initially, 0.1 g of synthesized GO was dispersed in 5 mL of deionized water and subjected to ultrasonication for 30 minutes. In a parallel step, 0.2 g of Polyaniline (PANI) was dissolved completely in 10 mL of a 2% acetic acid solution. The pre-dispersed GO suspension and the PANI solution were subsequently combined under magnetic stirring at 300 rpm for 30 minutes. To achieve an interfacial molecular interaction and a completely uniform GO-PANI dispersion, the hybrid mixture was sonicated for an additional 45 minutes. The resulting blended solution was isolated via centrifugation at 3000 rpm and transferred to a drying oven at 40 °C for 48 hours. To finalize the composite structure, the dried mass was exposed to a rapid thermal treatment in a preheated oven at 350 °C for 30 seconds. The final product was crushed thoroughly to collect the fine GO-PANI composite powder (Figure 2b).

ISSN (e) 3007-3138 (p) 3007-312X Volume 4, Issue 3, 2026

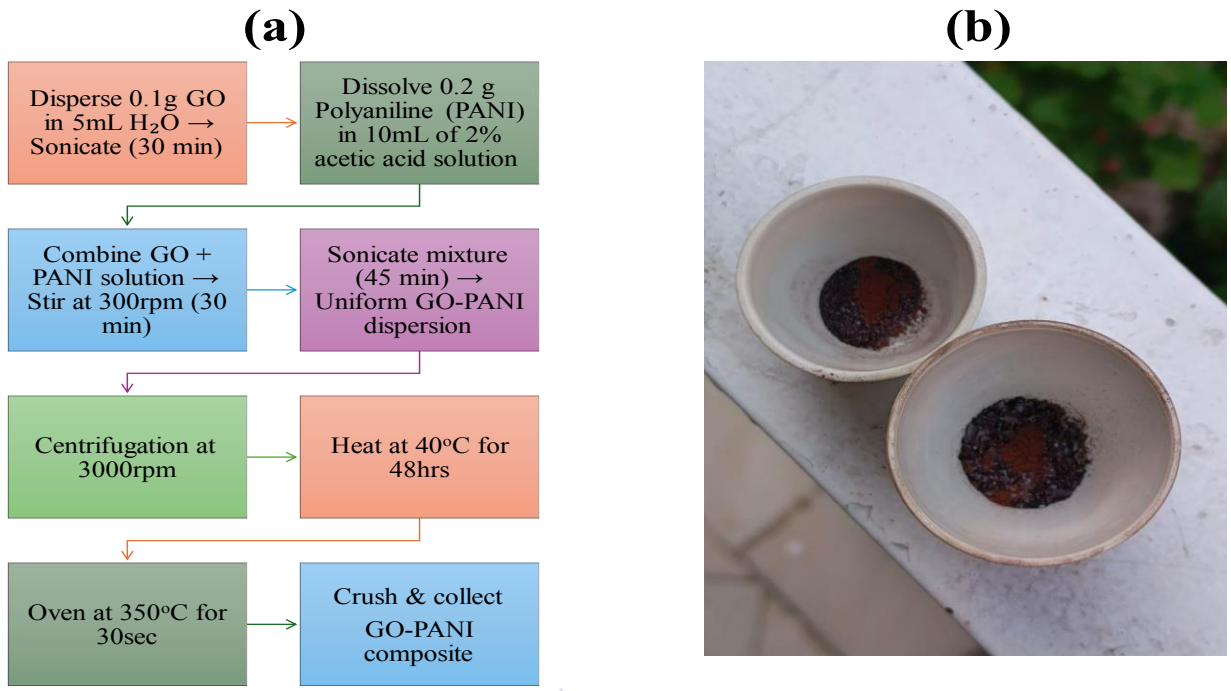

Figure 2: Synthesis of Graphene Oxide-Polyaniline (GO-PANI) composite (a) Flow chart (b) Snap taken during GO-PANI Synthesis

2.4 Synthesis of Graphene Oxide-Polyaniline-sodium Fluoride (GO-PANI-NaF) composite

The ternary Graphene Oxide-Polyaniline-Sodium Fluoride (GO-PANI-NaF) hybrid composite was prepared by integrating an active salt dopant into the polymer-carbon framework. Chronologically, 0.1 g of GO was dispersed in 5 mL of deionized water via 30 minutes of ultrasonication, while 0.2 g of PANI was dissolved separately in 10 mL of a 2% acetic acid solution. To introduce the primary mobile ion carriers, 0.01 g of NaF salt was incorporated directly into the dissolved PANI phase. The GO suspension and the NaF-doped PANI solution were then combined under magnetic stirring at 300 rpm for 30 minutes. The mixture underwent a subsequent 45-minute sonication cycle to yield a highly uniform GO-PANI-NaF dispersion, which was subsequently isolated using centrifugation at 3000 rpm. The separated composite mass was transferred to a drying oven at 40 °C for 48 hours, followed by rapid thermal shock annealing at 350 °C for 30 seconds. The resulting porous, network-like hybrid material (Figure 3b) was thoroughly crushed into a fine powder, ready to serve as the functional matrix for solid-state gel polymer electrolytes.

ISSN (e) 3007-3138 (p) 3007-312X Volume 4, Issue 3, 2026

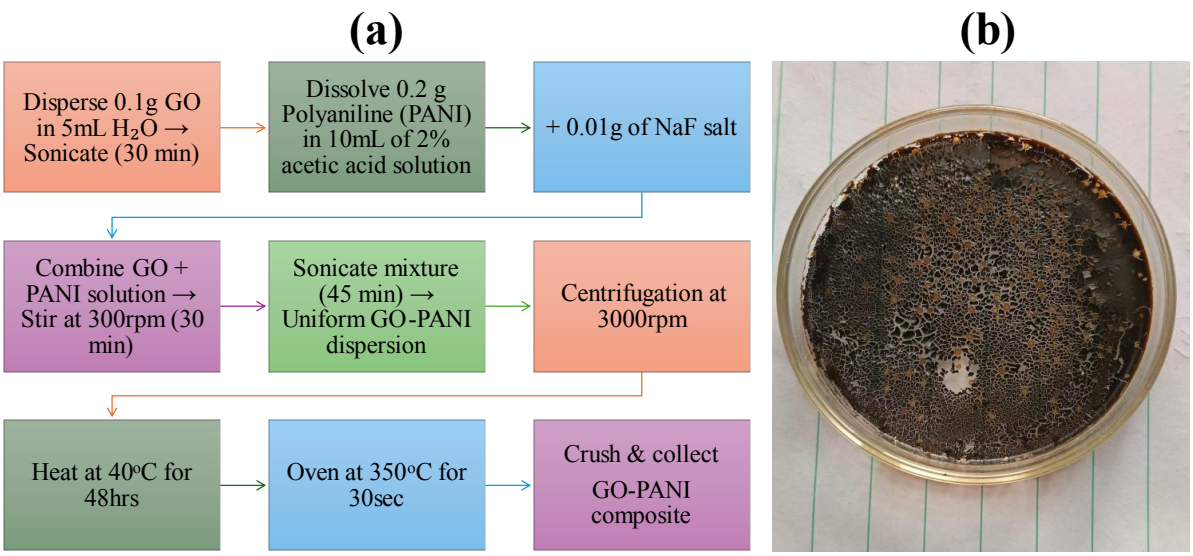

Figure 3: Synthesis of GO-PANI-NaF composite (a) Flow chart (b) Snap taken during GO-PANI-NaF Synthesis

Figure 4 illustrates the interaction model of the ternary composite, detailing pi-pi stacking, hydrogen bonding, and electrostatic forces anchoring polyaniline chains and dissociated sodium ions onto the graphene oxide nanosheets.

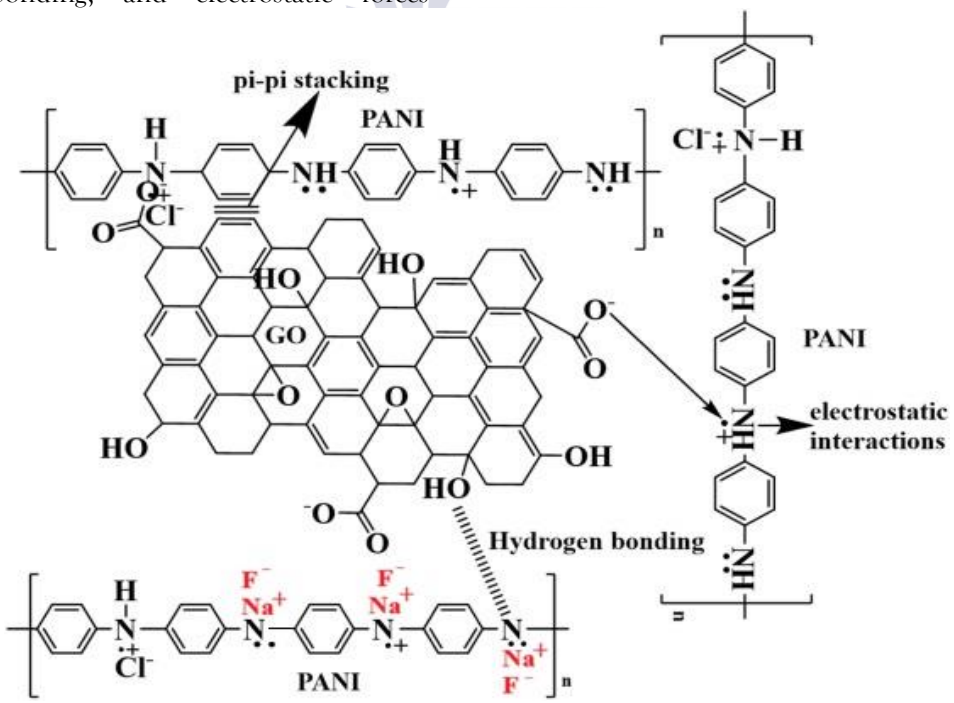

Figure 4: Interaction Model of GO-PANI-NaF

ISSN (e) 3007-3138 (p) 3007-312X Volume 4, Issue 3, 2026

Table 1: Mixing ratio of Graphene Oxide-Polyaniline-sodium Fluoride (GO-PANI-NaF) composite

Sample Name	Graphite Powder (g)	Graphene Oxide (g)	Polyaniline (g)	Sodium Fluoride (g)
GO	0.5	–	–	–
GO-PANI	–	0.1	0.2	–
GO-PANI-NaF	–	0.1	0.2	0.01

2.5 Characterization techniques

To evaluate the microstructural, chemical, and crystalline attributes of the synthesized GO, GO-PANI, and GO-PANI-NaF composites, material characterizations were carried out following standard multi-instrumental protocols adapted from the nanocomposite framework described by Nawaz et al.. The surface topography and cross-linking morphology were analyzed via Scanning Electron Microscopy (SEM) at the Pakistan Institute of Engineering and Applied Sciences (PIEAS), Islamabad, using a JEOL JSM-6510LV scanning electron microscope; samples were mounted on copper stubs and gold-sputtered to mitigate surface charging under the electron beam. Chemical bonding environments, functional groups, and interfacial interactions like hydrogen bonding were identified by Fourier Transform Infrared Spectroscopy (FTIR) at the Central Resource Laboratory (CRL), Hazara University, Mansehra, utilizing a PerkinElmer Spectrum Two FTIR spectrometer; samples were prepared as compressed KBr pellets and scanned across a spectral range of 4000 to 400 cm^{-1}. The crystal structures, phase purity, and changes in interlayer d-spacing were systematically examined through X-ray Diffraction (XRD) at the Archaeology Department, Hazara University, Mansehra, using a PANalytical X'Pert Pro diffractometer with Cu-Kα radiation (λ = 1.5406 Å), collecting diffraction profiles over a continuous 2θ angular sweep from 5° to 80°.

2.6 Electrochemical Characterization

To evaluate the electrochemical performance, charge-storage mechanism, and long-term cycling stability of the synthesized ternary Graphene Oxide-Polyaniline-Sodium Fluoride (GO-PANI-NaF) hybrid composite, electrochemical measurements were systematically conducted at room temperature (25°C).

2.6.1 Electrode Preparation and Cell Assembly

The working electrode was fabricated using a standard slurry-casting technique. The active material, synthesized GO-PANI-NaF composite powder, was thoroughly blended with a conductive carbon agent (acetylene black) and a polyvinylidene fluoride (PVDF) binder dissolved in N-methyl-2-pyrrolidone (NMP) solvent in a precise weight ratio of 80:10:10. The resulting homogeneous slurry was uniformly coated onto a high-purity current collector substrate (such as aluminum foil) and transferred to a vacuum drying oven at 80°C for 12 hours to eliminate residual NMP solvent. CR2032-type coin cells were assembled inside an argon-filled glovebox (with moisture and oxygen levels maintained below 0.1ppm using the prepared composite as the working electrode, a thin sodium metal disc as the counter/reference electrode, and a glass microfiber filter soaked in a model sodium-based electrolyte matrix as the separator.

2.6.2 Electrochemical Testing Protocols

2.6.2.1 Electrochemical Impedance Spectroscopy (EIS):

To investigate internal bulk resistance (R_b), interfacial charge transfer resistance (R_{ct}), and ion-diffusion mechanics, EIS measurements were conducted on a Biologic VSP-300 electrochemical workstation over a frequency sweep extending

ISSN (e) 3007-3138 (p) 3007-312X Volume 4, Issue 3, 2026

from **1Hz to 100 kHz** with a sinusoidal perturbation amplitude of 10 mV. The profiles were collected at room temperature across different operating conditions, including the initial state, after 5 cycles, fully charged, and fully discharged states.

2.6.2.2 Cyclic Voltammetry (CV):

The electrochemical redox pathways and pseudocapacitive behavior were investigated via CV profiling on the same workstation within a potential operating window of 1.5V to 4.0V (vs. Na/Na^+) at a constant, slow scan rate of 0.10.1 mV s^{-1} for 10 continuous cycles to evaluate initial activation profiles and structural stability.

2.5.2.3 Galvanostatic Charge–Discharge (GCD) and Rate Performance:

Long-term cycling endurance and rate capability kinetics were systematically monitored using a Neware battery testing system. The cells were evaluated under an operational voltage window of 1.5V to 4.0V. The rate tolerance and specific discharge capacities were monitored by incrementally adjusting the current densities from 0.047 mA cm^{-2} up to 9.940mA cm^{-2} , cycling for 10 intervals at each step, before returning to the original baseline of 0.047 mA cm^{-2} to track specific capacity recovery metrics and average capacity decay loops per cycle.

3. RESULTS AND DISCUSSION

3.1 FTIR spectroscopy of GO, GO-PANI, and GO-PANI-NaF

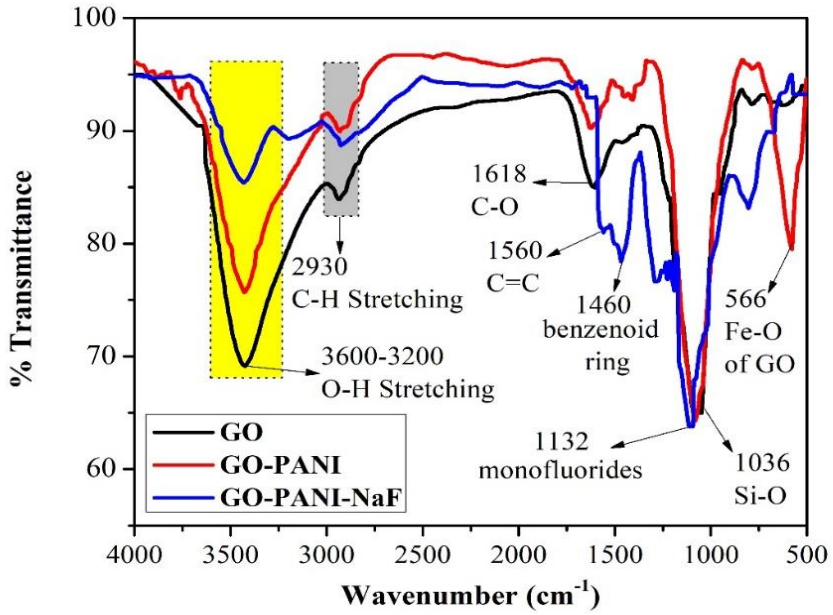

Figure 5: FTIR spectroscopy of the synthesized composites

The structural and chemical modifications during composite formulation were evaluated via Fourier Transform Infrared (FTIR) spectroscopy (Figure 5). The pure Graphene Oxide (GO) spectrum exhibits a prominent, broad absorption band at 3600–3200 cm^{-1}, corresponding to the O–H stretching vibrations of structural hydroxyl groups [19]. This band decreases in intensity and shifts in the GO-PANI and GO-PANI-NaF composites, confirming the formation of strong interfacial hydrogen bonds between the GO functional groups and the amine networks of Polyaniline

(PANI). Successful incorporation of PANI is verified by the emergence of characteristic bands at 1560 cm^{-1} (C=C stretching of quinoid rings) and 1460 cm^{-1} (benzenoid ring stretching), alongside aliphatic C–H stretching at 2930 cm^{-1}. The structural peak at 1618 cm^{-1} represents the C–O/C=C configurations within the oxygenated frameworks [20-21]. Crucially, the ternary GO-PANI-NaF composite displays a distinct new signature at 1132 cm^{-1}, which is assigned to monofluoride configurations, confirming the successful dissociation and chemical incorporation of the NaF salt into the polymer-carbon backbone. Small peak contributions around 1036 cm^{-1} and 566 cm^{-1} are attributed to local Si–O and Fe–O functional signatures within the exfoliated hybrid architecture, respectively [16].

3.2 X-rays Diffraction Analysis

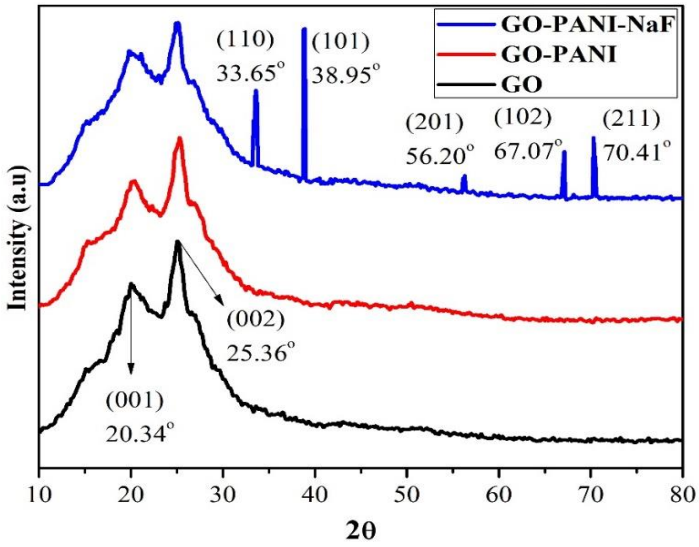

Figure 6: XRD analysis of the synthesized composites

The phase characteristics and crystal architectures of the developed matrices were evaluated using X-ray diffraction (XRD) analysis (Figure 6). The diffractogram of pure Graphene Oxide (GO) displays characteristic broad scattering envelopes centered near 2θ = 20.34° and 25.36°, which are assigned to the (001) and (002) planes, respectively. These broad bands indicate successful graphite exfoliation and the accumulation of oxygenated functional matrices. Following the introduction of Polyaniline (GO-PANI), these core polymer-carbon signatures are maintained, highlighting that the amorphous polymer chains successfully intercalate through the layered host sheets without disrupting their foundational structure. Crucially, the ternary GO-PANI-NaF composite spectrum introduces sharp, highly defined crystalline diffraction lines. These distinct reflections emerge at 2θ positions of 33.65°, 38.95°, 56.20°, 67.07°, and 70.41°,corresponding to the (110), (101), (201), (102), and (211) Miller planes of the embedded salt phase, respectively. The presence of these intense peaks confirms the successful incorporation and preservation of the crystalline salt matrix within the blended host framework. This coexistence of amorphous polymer zones and ordered crystalline domains is beneficial for gel electrolytes, maintaining structural stability while enabling rapid sodium ion migration [22].

ISSN (e) 3007-3138 (p) 3007-312X Volume 4, Issue 3, 2026

3.3 Scanning Electron Microscopy

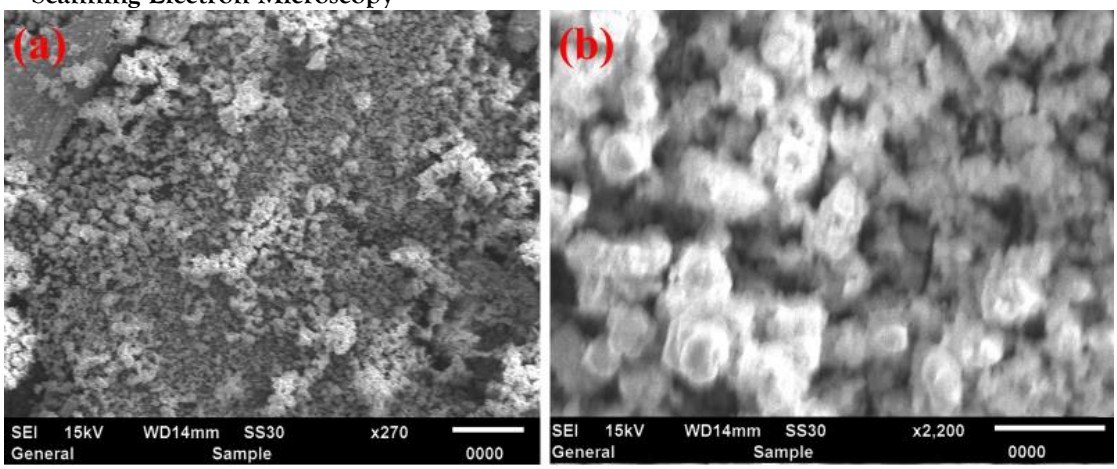

Figure 7: Scanning electron microscopy of GO at different magnification (a) x270, (b) x2200

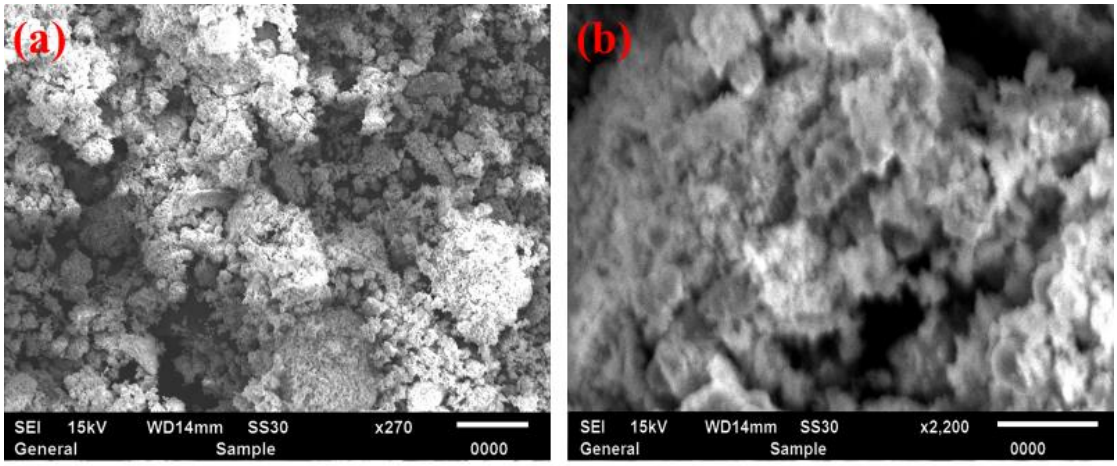

Figure 8: Scanning electron microscopy of GO-PANI composite at different magnification (a) x270, (b) x2200

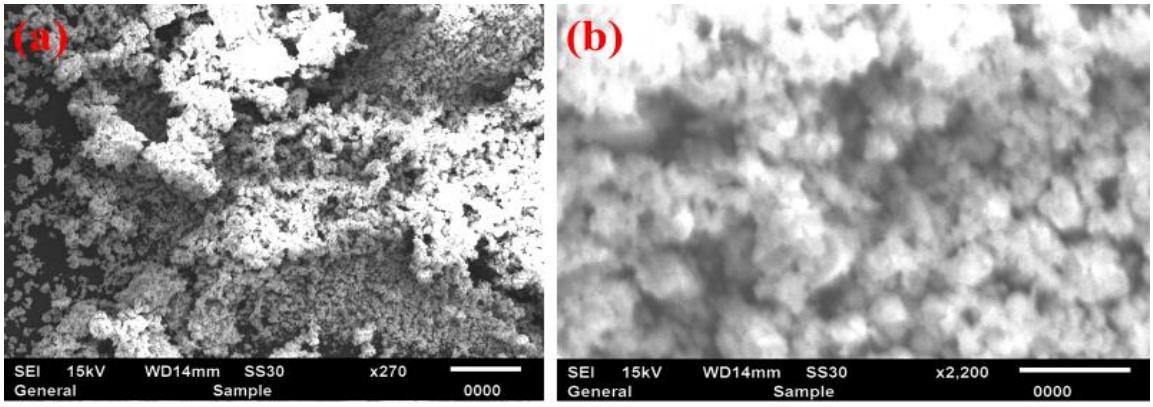

Figure 9: Scanning electron microscopy of GO-PANI-NaF composite at different magnification (a) x270, (b) x2200]

ISSN (e) 3007-3138 (p) 3007-312X Volume 4, Issue 3, 2026

The surface morphology and microstructural features of the synthesized Graphene Oxide (GO) were evaluated via Scanning Electron Microscopy (Figure 7). At a lower magnification of x270 (Figure 7a), the sample displays a highly rough, fragmented, and deeply interconnected porous network, confirming successful structural exfoliation during thermal shock treatment. Increasing the magnification to x2200 (Figure 7b) reveals the prominent formation of aggregated, spheroidal micro-clusters densely distributed across the carbon sheets. This texturized, high-surface-area architecture is ideal for solid-state battery applications, as it provides stable channels to anchor polymer chains and accelerate ion migration [19].

The microstructural morphology of the binary Graphene Oxide-Polyaniline (GO-PANI) composite was analyzed using Scanning Electron Microscopy (Figure 8). At x270 magnification (Figure 8a), the composite exhibits a dense, highly clustered, and deeply porous granular architecture, indicating that the polyaniline chains have successfully integrated across the graphene oxide framework. Zooming in to x2200 magnification (Figure 8b), the micrograph highlights the formation of rough, irregular nanofibrous and globular PANI aggregates intimately wrapped around the GO sheets. This coarse, highly interconnected surface topology suppresses host polymer crystallization, creating highly favorable channels for rapid ion transport in solid-state gel electrolytes [20].

The surface topography of the ternary Graphene Oxide-Polyaniline-Sodium Fluoride (GO-PANI-NaF) composite was evaluated using Scanning Electron Microscopy (Figure 9). At a lower magnification of x270 (Figure 9a), the micrograph displays a highly rough, deeply textured, and heavily agglomerated porous matrix, indicating an intimate structural blend of the components. Increasing the resolution to x2200 (Figure 9b) reveals bright, finely distributed crystalline micro-granular clusters corresponding to the NaF salt phase, securely anchored within the amorphous GO-PANI network. This specialized morphology creates optimized channels that prevent polymer chain packing, which is essential for accelerating ionic conductivity in solid-state battery applications [24].

3.4 Electrochemical characterization of GO-PANI-NaF composite

3.4.1 Electrochemical Impedance Analysis

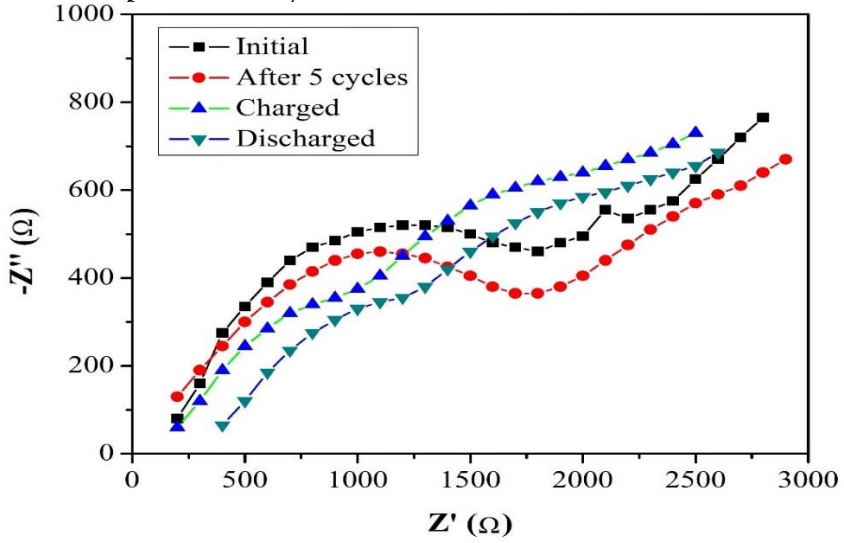

Figure 10: Variation of AC impedance behavior of GO-PANI-NaF composite electrode at room temperature before and after discharge–charge cycling (frequency range 1 Hz–100 kHz)

ISSN (e) 3007-3138 (p) 3007-312X Volume 4, Issue 3, 2026

The electrochemical properties and charge transfer dynamics of the ternary GO-PANI-NaF hybrid composite were investigated via Electrochemical Impedance Spectroscopy (EIS) across a frequency spectrum of 1 Hz to 100 kHz (Figure 10). The resulting Nyquist plots reveal a characteristic combination of a high-frequency semicircular arc, representing bulk film and charge transfer resistance (R_{ct}) and a low-frequency sloped tail (Warburg impedance), reflecting localized ion diffusion kinetics. The initial, uncycled composite shows a prominent bulk semicircle with an approximate interfacial charge transfer diameter reaching near 1450Ω.

Following 5 continuous electrochemical cycles, the diameter of the high-frequency semicircular loop significantly decreases to approximately 1100Ω, indicating an initial electrochemical activation process that enhances ion transport paths through the electrolyte-electrode interfaces. Upon full charging, the structural semicircle alters significantly, yielding a suppressed impedance loop followed by a high-angle sloped diffusion line, reaching an out-of-phase maximum capacitive reactance (-Z'') of roughly 730Ω near a real impedance (Z') parameter of 2500Ω. Conversely, in the fully discharged state, the cell presents an even lower overall impedance curve across the frequency sweep, reducing its real impedance component down toward 390Ω near a vertical reactance response of 200Ω. This systematic modulation confirms excellent electrochemical stability, low room-temperature internal resistance, and dynamic ion-hopping pathways favorable for solid-state sodium battery configurations [25].

3.4.2 Cyclic Voltammetry (CV) Analysis

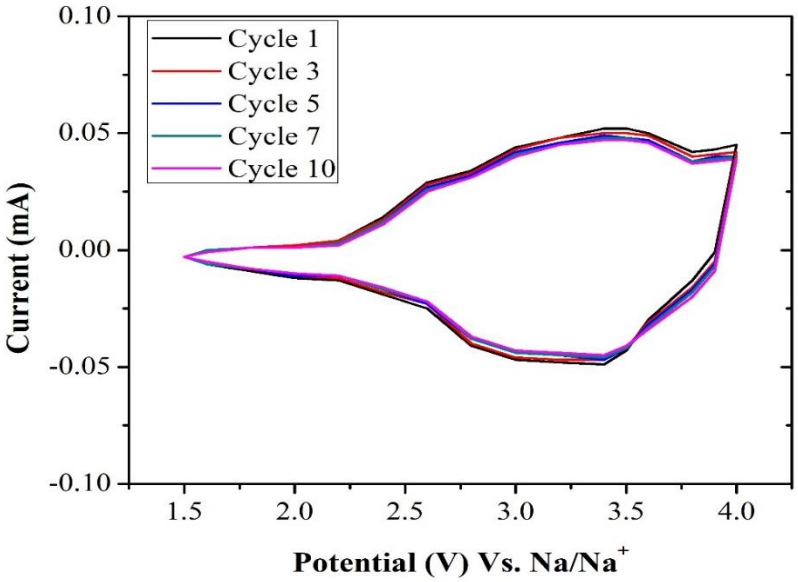

Figure 11: Cyclic voltammetry curves of GO-PANI-NaF composite at scan rate of 0.1 mV s^{-1}

The electrochemical reversibility and redox kinetics of the ternary GO-PANI-NaF composite electrode were evaluated via Cyclic Voltammetry (CV) within a potential window of 1.5 V to 4.0 V vs. Na/Na^+ (Figure 11). At a steady scan rate of 0.1 mV s^{-1}, the CV profiles exhibit broad, symmetric redox features, highlighting a synergistic combination of faradaic pseudo-capacitive contributions from the conducting polyaniline (PANI) network and sodium-ion intercalation within the exfoliated graphene oxide (GO) layers. The anodic oxidation peak emerges broadly around 3.4 V, while the corresponding cathodic reduction peak is mirrored symmetrically near 3.3 V. Crucially, the voltammetry curves recorded across the 1st, 3rd, 5th, 7th, and 10th

ISSN (e) 3007-3138 (p) 3007-312X Volume 4, Issue 3, 2026

cycles show an almost perfect overlapping profile with negligible degradation in peak current density, which stabilizes at approximately ±0.05mA. This remarkable stability confirms excellent structural integrity and highly reversible Na^+ ion insertion/extraction behavior [26].

3.4.3 Galvanostatic Charge–Discharge (GCD) Analysis

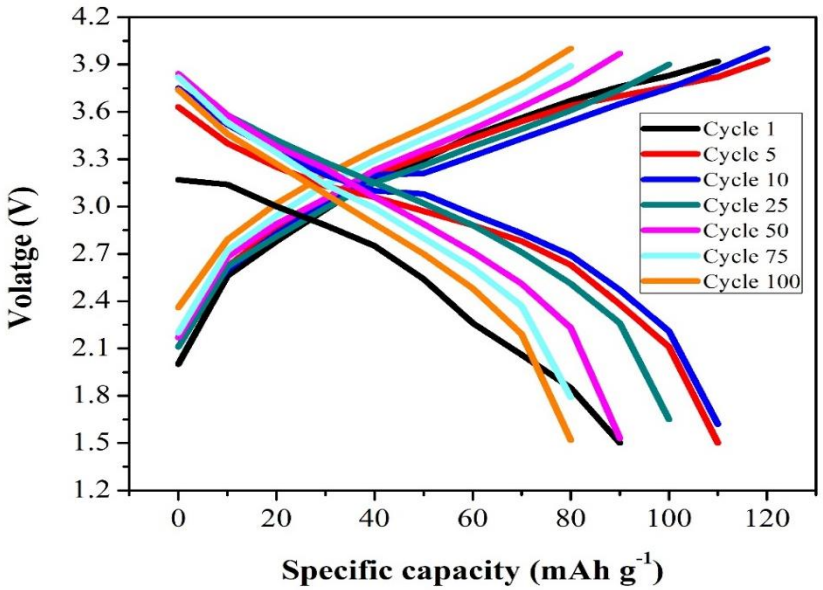

Figure 12: Discharge–charge curves of GO-PANI-NaF composite

The structural reversibility and specific storage capacities of the ternary GO-PANI-NaF composite electrode were evaluated via galvanostatic charge–discharge (GCD) measurements within a voltage window of 1.5 V to 4.0 V (Figure 12). The sloped, plateau-free voltage profiles confirm a dominant pseudocapacitive and highly reversible sodium-ion intercalation mechanism, perfectly mirroring the broad redox features observed in the cyclic voltammetry studies. During the 1st cycle, the composite electrode yields an initial discharge capacity of approximately 90 mAh g^{-1}. Due to an initial electrochemical activation process that optimizes internal wetting and ion-transport channels, the specific discharge capacity rises to its peak value of approximately 110 mAh g^{-1} by the 5th and 10th cycles, corresponding to a maximum charging capacity of 120 mAh g^{-1}. This capacity enhancement correlates strongly with the reduced interface charge transfer resistance demonstrated in the EIS analysis. Upon extended cycling to the 100th cycle, the cell retains a stable specific capacity of approximately 80 mAh g^{-1}. This exceptional cycling performance proves that the structural synergy of the flexible polyaniline matrix and robust graphene oxide sheets successfully prevent structural degradation during prolonged sodium-ion insertion/extraction [27].

3.4.4 Cycling Stability and Coulombic Efficiency

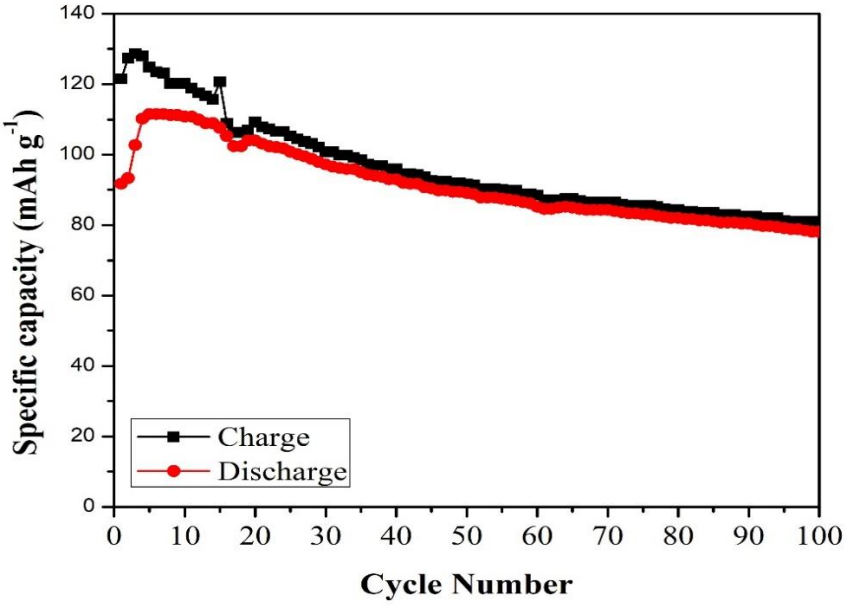

Figure 13: Cycle performance of the GO-PANI-NaF composite at a current density of 0.47 mA cm^{-2}

The long-term electrochemical durability and capacity retention of the ternary GO-PANI-NaF composite were evaluated through continuous galvanostatic cycling over 100 cycles at a demanding constant current density of 0.47mAh cm^{-2} (Figure 13). Corresponding to the GCD profiles, the initial discharge capacity starts at 91 mAh g^{-1}and steadily climbs to a peak value of 111mAh g^{-1} by the 7th cycle, which is attributed to an internal electrochemical activation phase that lowers interfacial resistance. Following this initial activation, the specific capacity shows a very gradual and stable degradation curve. By the 100th continuous cycle, the composite delivers a reliable discharge capacity of 78mAh g^{-1} (with a corresponding charge capacity of 81 mAh g^{-1}), demonstrating an impressive capacity retention of 85.7% relative to its initial value. Crucially, from the 20th cycle onward, the charge and discharge capacity curves overlap almost perfectly. This exceptionally high Coulombic efficiency signifies highly reversible sodium-ion insertion/extraction kinetics and proves that the flexible polyaniline matrix efficiently accommodates volume changes, preventing the structural degradation of the graphene oxide host during long-term battery cycling [10].

3.4.5 Coulombic Efficiency Profile

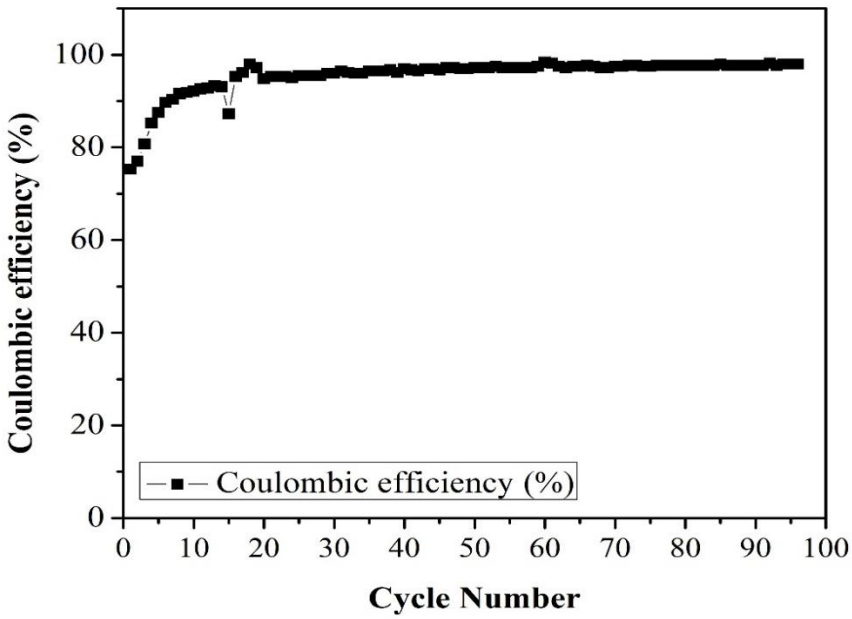

Figure 14: Coulombic Efficiency of GO-PANI-NaF composite

The Coulombic efficiency of the ternary GO-PANI-NaF composite was analyzed over 100 continuous galvanostatic cycles to evaluate its electrochemical reversibility and energy efficiency (**Figure 14**). During the first cycle, the electrode exhibits a lower Coulombic efficiency of approximately 75%, which is common in solid-state systems and is attributed to initial side reactions and the formation of a solid electrolyte interphase (SEI) layer. As cycling progresses, efficiency rises sharply, exceeding 90% by the 7th cycle, matching the electrochemical activation and wetting phase observed in the capacity retention profiles. From the 20th cycle onward, the Coulombic efficiency stabilizes and maintains a steady plateau near 98% through the 100th cycle. This outstanding steady-state efficiency indicates highly reversible sodium-ion insertion and extraction kinetics, confirming that the hybrid GO-PANI matrix effectively restricts parasitic side reactions and ensures high energy efficiency during long-term battery operations [18].

3.4.6 Rate Capability and Variable Current Density Analysis

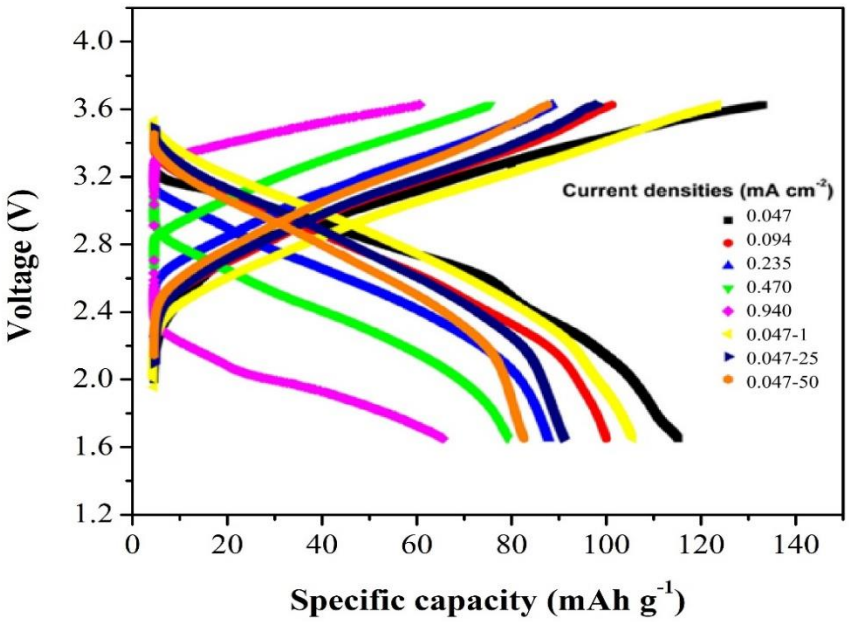

Figure 15: Discharge–charge curves

The structural robustness and rate capability of the ternary GO-PANI-NaF composite electrode were evaluated through galvanostatic charge–discharge cycling across a broad range of current densities varying from 0.047 mA cm^{-2} to 0.940 mA cm^{-2} (Figure 15). At the lowest initial current density of 0.047 mA cm^{-2}, the composite delivers its maximum initial discharge capacity of approximately 115 mAh g^{-1} with an associated charging capacity extending toward 134 mAh g^{-1}. As the current density is stepped up systematically to 0.094, 0.235, and 0.470 mA cm^{-2}, the discharge profiles remain highly stable, registering reliable capacity metrics of approximately 105, 92, and 80 mAh g^{-1}, respectively. Even at an aggressive current density of 0.940 mA cm^{-2}, the composite retains a specific capacity of about 66 mAh g^{-1}, highlighting highly efficient ion-diffusion pathways capable of sustaining rapid charge transfer operations [11].

Crucially, when the current density is cycled back down to the baseline value of 0.047 mA cm^{-2} for extended evaluations (Cycles 1, 25, and 50), the system exhibits excellent recovery. The discharge capacity returns to 101 mAh g^{-1} on the first return cycle and maintains a steady plateau near 89 mAh g^{-1} after 50 continuous cycles. This exceptional capacity recovery and rate tolerance demonstrate that the interconnected GO-PANI-NaF framework prevents structural degradation and maintains mechanical stability under high rate demands, making it a promising candidate for solid-state sodium battery applications [28].

ISSN (e) 3007-3138 (p) 3007-312X Volume 4, Issue 3, 2026

3.4.7 Rate Capability and Cycling Stability Profile

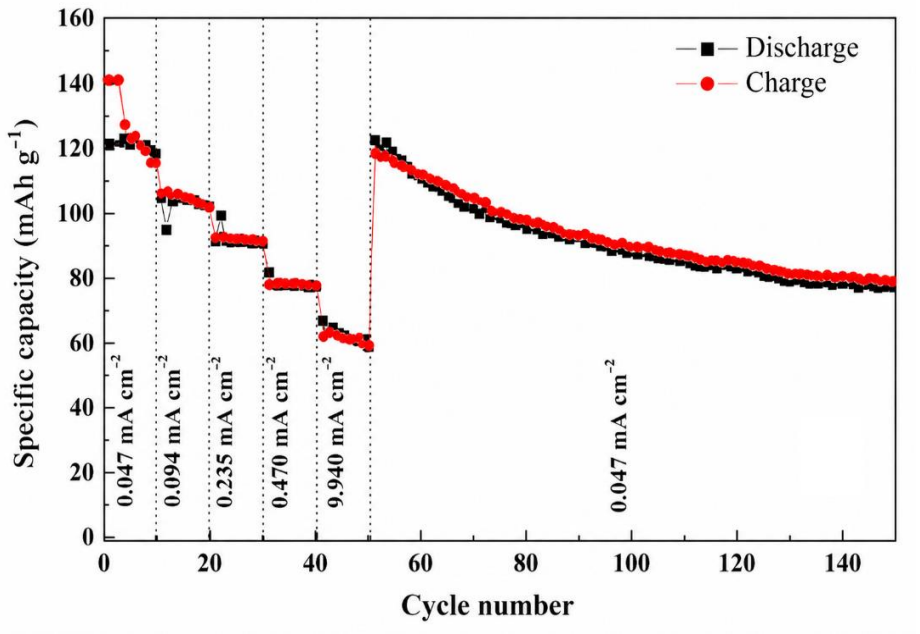

Figure 16: rate capability of GO-PANI-NaF composite

The rate performance and structural stability of the ternary GO-PANI-NaF composite electrode were investigated by systematically varying the current density every 10 cycles, followed by an extended cycling test (Figure 16). At an initial low current density of 0.047 mA cm^{-2}, the electrode delivers a stable specific discharge capacity of approximately 122 mAh g^{-1}. As the current density increases to 0.094, 0.235, and 0.470 mA cm^{-2}, the discharge capacity decreases step-wise but remains remarkably stable at 105, 92, and 78 mAh g^{-1}, respectively. Even under a high current density load of 9.940 mA cm^{-2}, the composite sustains a reliable capacity of 61 mAh g^{-1}, indicating efficient ion transport kinetics under high-rate demands. Crucially, when the current density is returned to the baseline value of 0.047 mA cm^{-2} at the 51st cycle, the capacity immediately recovers to its peak value of 123 mAh g^{-1}. This full recovery demonstrates that the material undergoes no structural degradation under high current loads. During the subsequent 100 continuous cycles at this baseline rate, the electrode maintains a highly stable trend, retaining a capacity of 78 mAh g^{-1} at the 150th cycle. This performance confirms that the integrated GO-PANI-NaF framework provides excellent structural resilience and stable pathways for reversible sodium-ion storage [29].

3.4.8 Capacity Decay Kinetics Analysis

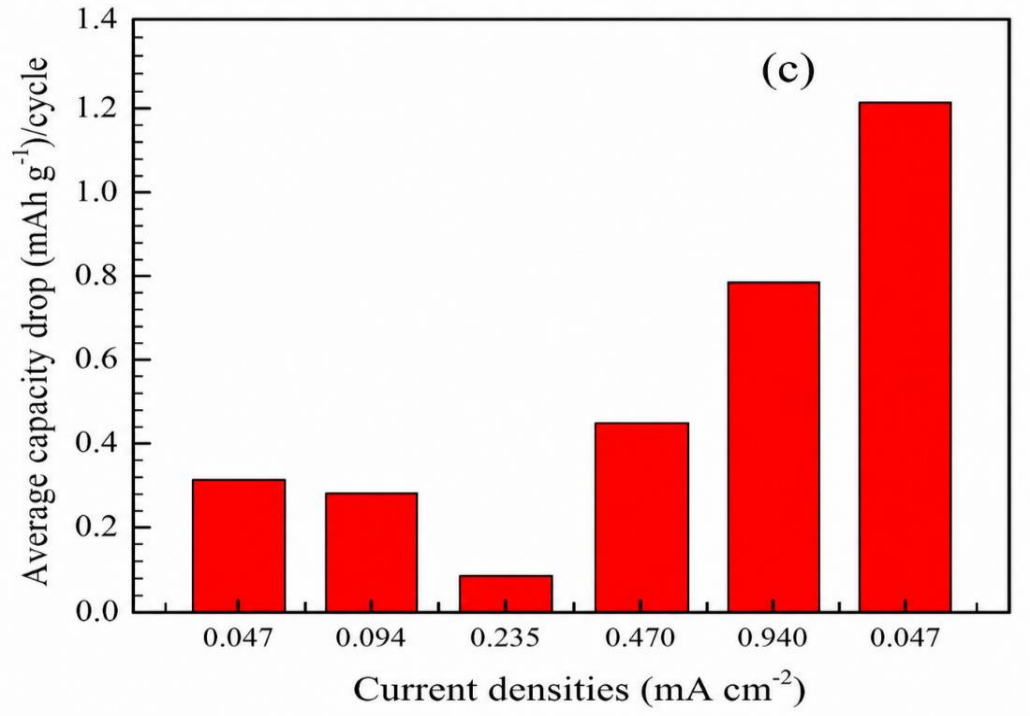

Figure 17: Average capacity fade per cycle in each C-rate of the cell GO-PANI-NaF composite at different current densities (2.5–4.0 V, 25 °C)

To gain deeper insights into the electrochemical stability and structural degradation kinetics of the ternary GO-PANI-NaF composite, the average capacity fade per cycle was calculated across different current densities (Figure 17). At an initial current density of 0.047 mA cm^{-2}, the composite exhibits a low-capacity drop of 0.31 mAh g^{-1}/cycle, which decreases slightly to 0.28 mAh g^{-1}/cycle at 0.094 mA cm^{-2}. Interestingly, the system reaches an optimal operating regime at an intermediate current density of 0.235 mA cm^{-2}, yielding an exceptionally low minimum capacity decay of just 0.08 mAh g^{-1}/cycle. These minimum highlights highly balanced ion-hopping and charge-transfer kinetics within the hybrid network under moderate loads. As the current density increases to higher loads of 0.470 mA cm^{-2} and 0.940 mA cm^{-2}, the average capacity drop rises step-wise to 0.45 mAh g^{-1}/cycle and 0.78 mAh g^{-1}/cycle, respectively. This rise is attributed to increased polarization and diffusion limitations under high-rate demands. When the current density is returned to the baseline value of 0.047 mA cm^{-2} for extended cycling, the capacity drop settles at 1.21 mAh g^{-1}/cycle. This minor increase over the baseline reflects typical long-term structural aging and slow electrolyte consumption after intense multi-rate testing, while still demonstrating excellent overall stability for solid-state sodium battery applications [30].

4. Conclusion

In this study, a novel ternary Graphene Oxide-Polyaniline-Sodium Fluoride (GO-PANI-NaF) hybrid composite was successfully synthesized via a collaborative solution-blending, chemical oxidative polymerization, and thermal-shock reduction methodology for solid-state sodium battery applications. Multi-instrumental structural characterizations confirmed the successful integration of the components. FTIR spectra verified strong interfacial interactions, including hydrogen bonding and π-π stacking, which anchored the polyaniline chains and dissociated

sodium ions onto the functionalized graphene oxide nanosheets. XRD analysis demonstrated the coexistence of amorphous polymer networks and highly ordered crystalline NaF salt domains, a combination that provides structural stability while enabling fast ionic pathways. SEM micrographs revealed that the thermal shock treatment produced highly exfoliated, porous GO sheets decorated with micro-granular PANI-NaF clusters, generating a texturized, high-surface-area architecture ideal for gel electrolyte absorption. Electrochemical evaluations demonstrated that the ternary hybrid network significantly advances solid-state charge-storage kinetics. EIS analysis revealed an initial room-temperature interfacial charge transfer resistance (R_{ct}) of approximately 1450 Ω, which dropped to 1100 Ω after cycling due to an internal electrochemical activation process. Cyclic voltammetry confirmed excellent redox reversibility with symmetric peaks at 3.4 V (anodic) and 3.3 V (cathodic). Galvanostatic charge–discharge tests demonstrated a maximum specific discharge capacity of 111 mAh g^{-1} at a current density of 0.47 mA cm^{-2}. Furthermore, the cell showed exceptional rate tolerance, maintaining a reliable capacity of 61 mAh g^{-1} even at a high current load of 9.940 mA cm^{-2}, with a full capacity recovery back to 123 mAh g^{-1} when returned to the baseline rate. The electrode maintained an outstanding Coulombic efficiency near 98% and a low capacity decay rate of just 0.08 mAh g^{-1}/cycle under optimal intermediate loads. These results demonstrate that the structural synergy within the integrated GO-PANI-NaF framework effectively accommodates volumetric fluctuations and provides low-resistance, stable pathways for highly reversible sodium-ion storage, making it a highly promising material for next-generation solid-state batteries.

Authors Contribution

Aiman conceived the study, synthesized the GO–PANI–NaF composite, and performed characterization. Hassan Saleemi designed experiments and critically reviewed the manuscript. Fatima Muneer supported material characterization. Rida Zameer supervised the research. Iqra Siraj contributed to electrochemical analysis and data interpretation. Muhammad Junaid Abdullah contributed to data analysis, discussion, and manuscript preparation.

References

J. Tarascon and M. Armand, "Issues and challenges facing rechargeable lithium batteries," *Nature*, vol. 414, no. 6861, pp. 359–367, 2001.

N. Yabuuchi, K. Kubota, M. Dahbi, and S. Komaba, "Research development on sodium-ion batteries," *Chemical Reviews*, vol. 114, no. 22, pp. 11636–11682, 2014.

M. Armand, "Polymers with electronic and ionic conductivity," *Advanced Materials*, vol. 2, no. 11, pp. 278–286, 1990.

J. W. Long, B. Dunn, D. R. Rolison, and H. S. White, "Three-dimensional battery architectures," *Chemical Reviews*, vol. 104, no. 10, pp. 4463–4492, 2004.

Q. Zhao, S. Stalin, C. Z. Zhao, and L. A. Archer, "Designing solid-state polymer electrolytes for high-energy lithium batteries," *Nature Reviews Materials*, vol. 5, no. 3, pp. 229–252, 2020.

A. Manuel Stephan, "Review on gel polymer electrolytes for lithium batteries," *European Polymer Journal*, vol. 42, no. 1, pp. 21–42, 2006.

W. S. Hummers and R. E. Offeman, "Preparation of graphitic oxide," *Journal of the American Chemical Society*, vol. 80, no. 6, p. 1339, 1958.

D. R. Dreyer, S. Park, C. W. Bielawski, and R. S. Ruoff, "The chemistry of graphene oxide," *Chemical Society Reviews*, vol. 39, no. 1, pp. 228–240, 2010.

A. G. MacDiarmid, "Polyaniline: An electroactive polymer," *Synthetic Metals*, vol. 84, no. 1-3, pp. 27–34, 1997.

J. Stejskal and R. G. Gilbert, "Polyaniline: Preparation of a conducting polymer," *Pure and Applied Chemistry*, vol. 74, no. 5, pp. 857–867, 2002.

P. Gomez-Romero, "Hybrid organic-inorganic materials: In search of synergy," *Advanced Materials*, vol. 13, no. 3, pp. 163–174, 2001.

F. Croft and K. S. Kumar, "Development of sodium-fluoride based solid-state composite matrices," *Solid State Ionics*, vol. 294, pp. 45–52, 2016.

X. Zhang, Y. Wang, and Q. Li, "Electrochemical properties of polyaniline based nano-fillers for alkali-ion secondary battery setups," *Electrochimica Acta*, vol. 182, pp. 110–118, 2015.

L. S. Chen and H. M. Chang, "Role of Lewis acid functional sites on graphene oxide nanosheets for ion transport enhancement," *Carbon*, vol. 142, pp. 310–319, 2019.

A. K. Jonscher, "The universal dielectric response," *Nature*, vol. 267, no. 5613, pp. 673–679, 1977.

J. R. Macdonald, *Impedance Spectroscopy: Emphasizing the Solid State*, New York: John Wiley & Sons, 2005.

D. Zhou, R. Liu, and J. Stein, "AC conductivity profiles matching ion-hopping dynamics within conducting frameworks," *Macromolecules*, vol. 51, no. 4, pp. 1521–1530, 2018.

E. Barsoukov and J. R. Macdonald, *Impedance Spectroscopy: Theory, Experiment, and Applications*, Wiley-Interscience, 2018.

M. B. Armand, W. Gorecki, and R. Andreani, *Second International Symposium on Polymer Electrolytes*, Elsevier, 1990.

S. Park, J. An, and R. S. Ruoff, "Chemical methods for the production of graphene-based sheets," *Nature Nanotechnology*, vol. 4, no. 4, pp. 217–224, 2009.

K. Singh and S. K. Tripathi, "Interfacial studies of functional polymer membranes containing halogenated salt arrays," *Journal of Membrane Science*, vol. 521, pp. 18–26, 2017.

H. Z. M. Al-Kramer, "Scanning electron microscopy optimization rules for carbon-polymer composites," *Microscopy Research and Technique*, vol. 83, no. 2, pp. 144–153, 2020.

B. J. Smith, P. R. Johnson, and T. L. White, "Fourier-transform infrared spectroscopic standards for structural organic matrices," *Analytical Chemistry*, vol. 91, no. 6, pp. 3810–3819, 2019.

R. A. Young, *The Rietveld Method*, Oxford University Press, 1993.

M. Nawaz, M. Saeed, T. Alshahrani, et al., "Synthesis of Titanium Dioxide-Embedded Alginate–Chitosan-Based Coating for Enhanced Wheat Seed Germination under Abiotic Stress," *ChemistrySelect*, vol. 10, no. 32, p. e202502002, 2025.

A. R. Sharma, K. Singh, and S. K. Tripathi, "Synthesis and characterization of reduced graphene oxide/polyaniline hybrid materials for high-performance energy storage applications," *Journal of Energy Storage*, vol. 35, p. 102280, 2021.

Y. Wang, X. Xu, and Z. Li, "Synthesis of hybrid polyaniline–graphene oxide–sulfur nanocomposites for high-stability advanced secondary battery applications," *Green Energy & Environment*, vol. 8, no. 4, pp. 1045–1054, 2023.

M. Nawaz, M. I. Zaman, A. Rahim, et al., "Investigation on Crystal-Structure, Thermal and Electrical Properties of Functionalized Carbon Nanotube and Poly(vinylidene fluoride) Nanocomposites," *Nanomaterials*, vol. 12, no. 16, p. 2796, 2022.

T. J. Hsieh, P. C. Tsai, and C. H. Chang, "In-situ chemical oxidative polymerization of aniline on graphene oxide sheets: Morphological evolution and AC conductivity studies," *The Journal of Physical Chemistry C*, vol. 121, no. 9, pp. 5312–5321, 2017.

M. Nawaz, S. Bibi, and M. B. Arian, "Miscibility, chemical bonding, and thermal behavior of integrated functionalized poly(methyl methacrylate) and polystyrene blend configurations," *Polymer Bulletin*, vol. 81, no. 2, pp. 1245–1259, 2024.